A comparison of three uncertainty calculus techniques for ultrasonic map building

Fabio Gambino Giuseppe Oriolo

Dipartimento di Informatica e Sistemistica
Università di Roma "La Sapienza"
Via Eudossiana 18, 00184 Roma, Italy
{gambino,oriolo}@labrob.ing.uniroma1.it

Giovanni Ulivi

Dipartimento di Discipline Scientifiche
Terza Università di Roma
Via della Vasca Navale, 84, 00146 Roma, Italy
ulivi@labrob.ing.uniroma1.it

ABSTRACT

Consider the problem of building the map of an unknown environment by using range readings obtained through ultrasonic sensors, and assume that a bitmap representation is adopted for compactness. In an ideal map, each cell of the bitmap is either empty or occupied by an obstacle. Because of the uncertainty introduced by sonar sensing, it is necessary to process appropriately the measures in order to classify each cell with a reasonable degree of accuracy. We compare three different algorithms for ultrasonic map building that are based respectively on Probability Theory, Fuzzy Logic and Fuzzy Measures. Simulation results in a one-dimensional case and experimental results for an office-like environment are presented to perform a comparison among the presented approaches.

Keywords: Map building, ultrasonic sensors, fuzzy logic, fuzzy measures, probability theory

1 INTRODUCTION

To perform navigation tasks in an unknown environment, a mobile robot needs to gather some information about the surrounding area through its on-board sensory system. Often, it is advisable to convey this knowledge into some sort of map. Due to its efficiency, a widely used representation is a bitmap of the free and the occupied space. Should the sensors behave ideally, the synthesis of a map building method would present no conceptual difficulty. Unfortunately, this assumption is never verified in practice and, on the contrary, many mobile robot sensors are cheap units that are prone to several kinds of errors.

A typical device in the above category is the ultrasonic sensor, whose performance may be rather poor due to various phenomena[1] (multiple reflections, wide radiation cone, etc.). As a consequence, the ultrasonic sensing process is affected by a large amount of uncertainty that is quite difficult to model, bewildering the engineer who must choose the right methodology for coping with uncertainty in the map building system.

Indeed, various approaches have been tried in the literature. Chronologically, the first has been the probabilistic approach[2] which found its definitive formulation[3] through the use of Bayesian techniques. To avoid some conceptual difficulties of this technique, we have successfully applied methodologies based on fuzzy logic.[4–6] Another possibility is to use the theory of fuzzy measures,[7] i.e., the Dempster-Shafer uncertainty calculus, that has already been used for processing stereo images from video cameras.[8]

However, each technique for dealing with uncertainty has its pros and cons,[9–11] and it may be quite arduous to select the most appropriate on a pure theoretical basis. Hence, we have decided to perform a field test in a real office-like environment, implementing with the greatest possible care three map building systems based on the aforementioned approaches.

The objective of this paper is to report on each implementation and to compare the relative results. For sake of clarity, in addition to experimental maps, we have included a simulated one-dimensional case, which allows to highlight the differences among the three methods. It should be emphasized that the significance of the performed tests is limited to the problem of ultrasonic map building; no general ranking is implied. Besides, since it appears impossible to assign a realistic performance criterion to a map building system, no 'optimization procedure' can be carried out during its synthesis. Therefore, we cannot exclude the possibility of improving the obtained results by using another implementation or different parameters.

2 PROBLEM FORMULATION

Consider a two-dimensional environment and assume that, for computational reasons, a discretized representation consisting of a bitmap U of square cells is adopted. A series of range readings $\{r_1, \ldots, r_n\}$ collected at known sensor locations is available[†]. In principle, the task of the Map Building System (MBS) should be to process the measures in order to determine, as accurately as possible, which cells are (even partially) occupied by obstacles and which cells are (completely) empty and thus suitable for robot navigation; no other characterization of the cells is of interest. In view of this, the *power set* $\Psi(U)$ of the *universal set* U contains the set of the empty cells E, the set of the occupied cells $O = \bar{E}$, the universal set U itself and the empty set $\emptyset$.

Due to the presence of uncertainty, the MBS will only be able to provide an 'estimate' of which cells belong to E and which ones belong to O. A compact way to represent this estimate is through a *gray-level* navigation map $\mathcal{N}$, in which each cell c of U is characterized by a real number $\nu(c) \in [0, 1]$ summarizing the information on c gathered from $\{r_1, \ldots, r_n\}$. The interpretation as well as the computation of ν depend on the particular method chosen for managing uncertainty. In this paper, we shall examine three approaches for processing ultrasonic measures, namely Probability Theory (PT), Fuzzy Logic (FL) and Fuzzy Measures (FM).

With the PT approach,[3] the map $\mathcal{N}$ is obtained by letting

$$\nu(c) = P(c \in O \,|\, \{r_1, \ldots, r_n\}),$$

i.e., the conditional probability that c is occupied given the sensor range readings $\{r_1, \ldots, r_n\}$. Being E and O complementary sets, the above probability is our best estimate about the possible state of cell c (empty or occupied).

A different trend of thought[4] must be pursued in order to cast the map building problem in a FL context. In particular, one may try to quantify the degree of belief of the assertions 'cell c belongs to set E' and 'cell c belongs to set O'. This situation can be modeled by regarding the two sets of empty and occupied cells as *fuzzy* sets, respectively $\mathcal{E}$ and $\mathcal{O}$ (as opposed to the *crisp* sets E and O), thus letting their membership functions $\mu_{\mathcal{E}}$ and $\mu_{\mathcal{O}}$ assume any value in the continuous interval $[0, 1]$. With this approach, the *tertium non datur* axiom does not hold: the same cell c can partially belong to both $\mathcal{E}$ and $\mathcal{O}$. This peculiarity of the approach proves to be particularly useful in the presence of ambiguous information, allowing to compute the fuzzy set $\mathcal{D}$ of the *dangerous* cells by properly combining $\mathcal{E}$ and $\mathcal{O}$. The navigation map $\mathcal{N}$ is then defined as

$$\nu(c) = \mu_{\mathcal{D}}^{\{r_1, \ldots, r_n\}}(c),$$

i.e., the membership function of cell c to the fuzzy set $\mathcal{D}$, with the latter computed on the basis of the sensor measures $\{r_1, \ldots, r_n\}$.

[†]The problem of selecting the sensor locations is outside the scope of this paper.

Another appealing technique to derive evidence in support of two (or more) possible alternatives is based on the use of the fuzzy measures theory.[7] As this approach is somewhat non-standard, we shall briefly recall some basic concepts below*.

A *fuzzy measure* is defined by a function

$$g:\ U \times \Psi(U) \mapsto [0,1].$$

For each cell c and each crisp subset X of U, $g_X(c)$ represents the degree of available evidence that c belongs to X. A fuzzy measure must satisfy four axioms about boundary conditions, monotonicity, continuity and additivity. The two fundamental fuzzy measures are the Belief function and its dual, the Plausibility function. Both can be expressed in terms of a single function m_X, called Basic Probability Assignment (BPA), such that

$$m:\ U \times \Psi(U) \mapsto [0,1], \qquad \sum_{X\in\Psi(U)} m_X(c) = 1.$$

In particular, Belief and Plausibility functions are defined as

$$\mathrm{Bel}_X(c) = \sum_{Y\in\Psi(U):Y\subseteq X} m_Y(c), \qquad \mathrm{Pl}_X(c) = \sum_{Y\in\Psi(U):X\cap Y\neq\emptyset} m_Y(c).$$

The duality between the two functions is expressed by

$$\mathrm{Pl}_{\bar{X}}(c) = 1 - \mathrm{Bel}_X(c).$$

For the application to ultrasonic map building, we must specify how the sensor readings are processed in order to obtain for each cell c of U the BPA. The first three functions of this assignment are $m_E(c)$, the degree of evidence that c is empty, $m_O(c)$, the degree of evidence that c is occupied, and $m_U(c)$, the degree of evidence that c is nothing more than a member of U. The value of $m_\emptyset(c)$ is always zero with the standard Dempster-Shafer theory, that assumes a *closed-world* in which the possible states of a cell are only empty and occupied. The BPA is updated on the basis of the sensor measures $\{r_1,\ldots,r_n\}$ by using the Dempster-Shafer rule.

A first reasonable choice for the definition of the navigation map $\mathcal{N}$ could be

$$\nu(c) = \mathrm{Pl}_O(c) = 1 - \mathrm{Bel}_E(c) = 1 - \mathrm{m}_E(c),$$

i.e., the plausibility that cell c is occupied. However, with this approach the information contained in $\mathrm{Bel}_O(c)$ is not conveyed into $\mathcal{N}$, resulting in an overconservative map. A better alternative is to apply the so-called *pignistic* approach[12]

$$\nu(c) = \frac{1}{2}\,(\mathrm{Pl}_O(c) + \mathrm{Bel}_O(c)) = \mathrm{m}_O(c) + \frac{1}{2}\,\mathrm{m}_U(c),$$

in which the 'bet' is placed on the basis of the mean value between favorable and unfavorable odds.

3 UNCERTAINTY MODELS FOR ULTRASONIC SENSING

Ultrasonic rangefinders are widely used for measuring relative distances, due to their low cost and simplicity of operation. The working principle is very simple: a packet of ultrasonic waves transmitted by the emitter is reflected by obstacles, originating an echo that is detected by the receiver. The time elapsed between transmission and reception determines the distance of the obstacle.

For illustration, we refer to the Polaroid Ultrasonic Rangefinder,[13] a very common device that can detect distances in the range 0.12÷6.5 m with 1% accuracy. The multi-lobed power diagram of the transmitter may be obtained from the radiation directivity function of a plane circular piston

$$D(\vartheta) = 2\frac{J_1(k\eta\sin\vartheta)}{k\eta\sin\vartheta}, \tag{1}$$

*We shall make use of a notation slightly modified w.r.t. the canonical one in view of the application to map building.

where $J_1(\cdot)$ is the Bessel function of the first order, $k = 2\pi/\ell$ depends on the wavelength ℓ, η is the piston radius and ϑ is the azimuthal angle measured with respect to the beam central axis. For the Polaroid sensor it is $\eta = 0.01921$ m and $\ell = v/\varphi$, where v is the sound speed in air and $\varphi = 49.410$ kHz. In practice, it is sufficient to take into account only the principal lobe of the pattern, and consider the waves to be diffused over a radiation cone of 25° width.

An ultrasonic sensor is far from being an ideal sensor, mainly due to the width of the radiation cone and to the multiple reflections phenomenon. The former does not allow to determine the exact angular position of the obstacle on the 25° arc of circle corresponding to the detected distance. The latter needs a more thorough explanation. Incident ultrasonic waves are reflected in two different ways depending on the surface irregularities of the surface. If their size is much smaller than the wavelength of the ultrasonic signal, we have a diffused reflection, i.e., the incident energy is scattered in all directions; otherwise, the reflection is mainly specular and the beam may either reach the receiver after multiple reflections or even get lost. Therefore, in order to return a significant range reading, the angle of incidence on the object surface has to be smaller than a critical angle, which depends on surface characteristics. Typical values range from 7–8° for smooth glass to almost 90° for very rough materials.

In the remainder of this section, we shall see how the above qualitative description can be used to set up an uncertainty model for ultrasonic sensing in the PT, FL and FM approaches. In particular, while the last two share a common uncertainty model, the PT approach is based on a completely different description.

3.1 Probability Theory

With the PT approach, the sensor uncertainty model is given as a probability density function $p(r|\rho,\vartheta)$, which characterizes the probability of measuring r provided that the obstacle closest to the sensor is located at (ρ,ϑ) inside the radiation cone.

If the sensor behavior were ideal, $p(r|\rho,\vartheta)$ would be an impulse function centered at (ρ,ϑ). In practice, a two-dimensional gaussian distribution is often adopted to account for uncertainty. To improve the model accuracy in the presence of multiple reflections, it is advisable to 'shape' the gaussian distribution depending on the value of r and ρ. In particular, it has been suggested[3] to increase the radial variance σ_ρ linearly with r, while letting the amplitude be itself a gaussian function of ρ, centered at an optimal detection distance R_m. The rationale for the first choice is that larger amounts of uncertainty are typically associated to longer distance readings. As for the second, it relies on the simple consideration that the farther the obstacle is from R_m, the less is the probability to detect it.

Therefore, the following sensor uncertainty model can be used:

$$p(r|\rho,\vartheta) = p_a(\rho)\left(\frac{1}{\sqrt{2\pi}\sigma_\rho}e^{-\frac{(r-\rho)^2}{2\sigma_\rho^2}}\right)\left(\frac{1}{\sqrt{2\pi}\sigma_\vartheta}e^{-\frac{\vartheta^2}{2\sigma_\vartheta^2}}\right), \qquad p_a(\rho) = \frac{1}{\sqrt{2\pi}\sigma_a}e^{-\frac{(\rho-R_m)^2}{2\sigma_a^2}}, \quad \sigma_\rho = h_1 r + h_2, \tag{2}$$

where h_1, h_2 are constants. The variances σ_a and σ_ϑ should be determined from the specific sensor characteristics.

3.2 Fuzzy logic and fuzzy measures

A range reading r provides the information that one or more obstacles are located somewhere along the 25° arc of circumference of radius r. Hence, there is evidence that cells located in the proximity of this arc are 'occupied'. On the other hand, cells well inside the circular sector of radius r are likely to be 'empty'. To model this knowledge, we introduce the two functions

$$f_e(\rho,r) = \begin{cases} k_e & 0 \le \rho < r-\Delta r \\ k_e\left(\frac{r-\rho}{\Delta r}\right)^2 & r-\Delta r \le \rho < r \\ 0 & \rho \ge r, \end{cases} \qquad f_o(\rho,r) = \begin{cases} 0 & 0 \le \rho < r-\Delta r \\ k_o\left[1-\left(\frac{r-\rho}{\Delta r}\right)^2\right] & r-\Delta r \le \rho < r+\Delta r \\ 0 & \rho \ge r+\Delta r, \end{cases} \tag{3}$$

that describe, respectively, how the degrees of certainty of the assertions 'empty' and 'occupied' vary with the distance ρ of the cell c from the sensor, for a given range reading r. Here, k_e and k_o are two constants and $2\cdot\Delta r$ is the width of the area considered 'proximal' to the arc of radius r.

Since the intensity of the waves decreases to zero at the borders of the radiation cone, the degree of certainty of each assertion should be higher for cells close to the beam axis. This is realized by means of the following function

$$f_a(\vartheta) = \begin{cases} D(\vartheta) & 0 \le |\vartheta| \le 12.5^\circ \\ 0 & |\vartheta| > 12.5^\circ, \end{cases} \tag{4}$$

where $D(\vartheta)$ is the radiation directivity function (1).

Finally, a third function is introduced in order to weaken the confidence of each assertion as the distance from the sensor increases

$$f_d(\rho) = 1 - \frac{1 + \tanh\bigl(2(\rho - \rho_v)\bigr)}{2}. \tag{5}$$

The parameter ρ_v plays the role of a 'visibility radius', i.e., a distance at which a smooth transition occurs from certainty to uncertainty. The motivation for introducing this function is twofold. First, as multiple reflections give often rise to 'long' readings, the use of $f_d(\rho)$ reduces the effect of erroneous measures on the map building process. Besides, narrow passages and doors appear to be obstructed if seen from a large distance, due to the sensor wide radiation angle. By varying the visibility radius according to the characteristics of the environment, it is possible to obtain a more correct detection behavior.

4 MAP BUILDING ALGORITHMS

The common objective of the three map building algorithms (PT, FL, FM) presented below is to produce the navigation map $\mathcal{N}$ by processing the range readings $\{r_1, \ldots, r_n\}$ on the basis of the appropriate uncertainty model.

4.1 Probability theory

The probabilistic approach is based on the recursive application of Bayes Theorem to obtain the occupancy probability of each cell after a range reading r

$$P\,[c \in O \,|\, \{r_1, \ldots, r_n\}] = \frac{p\,[r_n \,|\, c \in O]\, P\,[c \in O \,|\, \{r_1, \ldots, r_{n-1}\}]}{p\,[r_n \,|\, c \in E]\, P\,[c \in E \,|\, \{r_1, \ldots, r_{n-1}\}] + p\,[r_n \,|\, c \in O]\, P\,[c \in O \,|\, \{r_1, \ldots, r_{n-1}\}]}.$$

In this formula:

- $p\,[r_n \,|\, c \in X]$ (for $X = E, O$) is obtained through the application of Kolmogorov theorem

  $$p\,[r_n \,|\, c \in X] = \sum_{G(X)} p[r_n \,|\, G(X), c \in X]\, p[G(X) \,|\, c \in X],$$

  where $G(X)$ is the set of possible configurations (empty/occupied) of the bitmap compatible with the assumption that c belongs to X. Here, one makes use of the probability density function $p[r \,|\, \rho, \vartheta]$ to derive $p[r_n \,|\, G(X), c \in X]$. The above operation can be interpreted as a sort of weighted mean of the probability density function—the sensor uncertainty model—over the possible locations of the obstacle in U. To keep the computation viable—although cumbersome—one must assume a zero-order Markov field, i.e., that no relationship exists between the states of two cells, even if they are adjacent.

- $P\,[c \in X \,|\, \{r_1, \ldots, r_{n-1}\}]$ (for $X = E, O$) are the previous estimates of the cell state. For $n = 1$, it is necessary to use the *a priori* estimates $P[c \in E]$ and $P[c \in O]$, satisfying the constraint $P[c \in E] + P[c \in O] = 1$. A typical choice is the *maximum entropy* assumption, i.e., $P[c \in E] = P[c \in O] = 1/2$.

4.2 Fuzzy logic

By combining the certainty functions (3–5), it is possible to generate the two membership functions

$$\mu_{\mathcal{E}}^{\{r\}} = f_e(\rho, r) f_a(\vartheta) f_d(\rho), \qquad \mu_{\mathcal{O}}^{\{r\}} = f_o(\rho, r) f_a(\vartheta) f_d(\rho),$$

which define respectively the fuzzy sets $\mathcal{E}^{\{r\}}$ (empty cells) and $\mathcal{O}^{\{r\}}$ (occupied cells) inside the radiation cone, on the basis of the range reading r. Here, ρ and ϑ are the polar coordinates of the generic cell w.r.t. the sensor position.

As new range readings are collected, they are used to update the fuzzy sets by using a fuzzy *union* operator:

$$\mathcal{E}^{\{r_1,\ldots,r_{i+1}\}} = \mathcal{E}^{\{r_1,\ldots,r_i\}} \cup \mathcal{E}^{\{r_{i+1}\}}, \qquad \mathcal{O}^{\{r_1,\ldots,r_{i+1}\}} = \mathcal{O}^{\{r_1,\ldots,r_i\}} \cup \mathcal{O}^{\{r_{i+1}\}}.$$

Note that complete ignorance is assumed at the beginning, meaning that $\mu_{\mathcal{E}}$ and $\mu_{\mathcal{O}}$ are identically zero at the beginning for all cells (i.e., $\mathcal{E}^{\emptyset} = \mathcal{O}^{\emptyset} = \emptyset$).

The gray-level bitmap $\mathcal{N}$ can be built by properly combining the two sets $\mathcal{E}$ and $\mathcal{O}$. In fact, they are *not* complementary, hence making possible to identify areas where the available information is either conflicting or insufficient. In particular, let

$$\mathcal{A} = \mathcal{E} \cap \mathcal{O}, \qquad \mathcal{I} = \bar{\mathcal{E}} \cap \bar{\mathcal{O}},$$

be respectively the fuzzy sets of *ambiguous* and *indeterminate* cells, with $\cap$ denoting a fuzzy *intersection* operator. The navigation map $\mathcal{N}$ coincides with the fuzzy set $\mathcal{D}$ of the *dangerous* cells, defined as

$$\mathcal{D} = \bar{\mathcal{S}}, \qquad \text{with} \qquad \mathcal{S} = \mathcal{E}^2 \cap \bar{\mathcal{O}} \cap \bar{\mathcal{A}} \cap \bar{\mathcal{I}},$$

i.e., as the complement of the set $\mathcal{S}$ of *safe* cells, obtained by 'discarding' the *occupied*, the *ambiguous* and the *indeterminate* cells from the *very empty* ones.

The reader can refer to many textbooks[7,14,15] for a review of fuzzy set operators. In our experience, convenient choices[4] are the Dombi[16] union and the bounded product[7] intersection, together with the standard complementation operator. The tuning of the parameters for these operators as well as for the certainty functions (3–5) can be made on the basis of a rough qualitative description of the environment.[4]

4.3 Fuzzy measures

In the same spirit of the FL approach, the basic probability assignment corresponding to a range reading r can be directly obtained through the certainty functions (3–5)

$$m^{\{r\}}(E) = f_e(\rho, r) f_a(\vartheta) f_d(\rho), \quad m^{\{r\}}(O) = f_o(\rho, r) f_a(\vartheta) f_d(\rho), \quad m^{\{r\}}(U) = 1 - m(E) - m(O), \quad m^{\{r\}}(\emptyset) = 0.$$

These assignments express the evidence that the cell located at (ρ, ϑ) belongs to the (crisp) sets E, O, U and $\emptyset$, respectively.

As more range readings become available, the above evidence is updated by using the Dempster-Shafer combination rule

$$m^{\{r_1,\ldots,r_{i+1}\}}(X) = \frac{\sum_{Y,Z\in\Psi(U):Y\cap Z=X} m^{\{r_1,\ldots,r_i\}}(Y)\, m^{\{r_{i+1}\}}(Z)}{1-K}, \qquad \forall X \in \Psi(U), X \neq \emptyset, \qquad m^{\{r_1,\ldots,r_{i+1}\}}(\emptyset) = 0,$$

being

$$K = \sum_{Y,Z\in\Psi(U):Y\cap Z=\emptyset} m^{\{r_1,\ldots,r_i\}}(Y) m^{r_{i+1}}(Z).$$

The computation is initialized at $m^{\emptyset}(E) = m^{\emptyset}(O) = 0$ and $m^{\emptyset}(U) = 1$, i.e., total ignorance.

5 COMPARISONS

The three map building algorithms have been implemented in C on a RISC 6000 workstation running under UNIX. Graphic postprocessing is performed in Mathematica.

5.1 Simulated maps

In order to obtain repeatable and easily readable results, a set of preliminary tests have been performed in a simulated one-dimensional environment. The cells are thus segments of size 0.1 m and the sensor, located at the origin, simply provides a series of numbers (distance readings). When the measure pattern consists of identical (or very similar) readings, all the methods behave well and accurately detect the empty and the occupied areas in front of the sensor. To simulate the presence of a multiple reflection, we have generated an input sequence $\{0.5, 0.5, 0.5, 0.5, 2\}$, in which the first four values represent the correct reading while the last acts as an outlier.

The results of the PT method (Fig. 1) are not satisfactory. The three curves (dotted, dashed and plain line) respectively show the map profile after the first, the fourth and the fifth iteration. While the first four readings build up occupancy probability ($\nu(c) > 0.5$) at 0.5 m, indicating the presence of an obstacle, such certainty is erased when the last reading is processed. Moreover, the area extending from the sensor to a distance of 1 m is assigned a high probability of emptiness.

The map generated by the FL method, drawn in Fig. 2, is more accurate. Recall that, with this approach, $\nu(C)$ represents the membership function of c to the fuzzy set of *dangerous* cells, i.e., the risk of navigating through c. Therefore, *indeterminate* cells are accounted for in $\mathcal{N}$, and the area behind the obstacle is assigned the same value of the obstacle edge. When the outlier is processed, this value is somewhat decreased, but the previous information about the presence of an obstacle at 0.5 m is retained.

Figure 3 shows the map obtained with the FM method, in which $\nu(c)$ represents an intermediate value between the plausibility and the belief that c is occupied. The values of $\mathcal{N}$ are low close to the sensor, where all the readings indicate the presence of an empty space. Cells around 0.5 m are characterized by high evidence of occupancy even if the fifth reading produces a small reduction. Cells behind the obstacle keep the initial indeterminacy for the first four measures, for they are never explored by the beam. Again, the outlier does not destroy the previously gathered information, a desirable feature lacking with the PT approach. Although the results are very similar to those of the FL method, the convergence of the latter seems to be faster.

Another important aspect to be analyzed is the behavior of the three map building algorithms in the presence of *conflicting* range readings. To represent this situation, we have used an alternating input sequence of values 0.5 m and 1.5 m. The obtained maps are not reported for lack of space. Here, we shall just say that the FL and FM methods provide a significant final map with two peaks, from which the anomalous situation can be detected. The PT method, on the contrary, is naturally apt to assume that the longest readings are more reliable, and thus no conflict can be found in the final map.

5.2 Experimental maps

As a field test, the three algorithms have been used in order to build a map of a rather large and complex environment, composed by a corridor of our department, the entrance and a room with an irregular shape. A small obstacle was positioned at the crossing between the entrance and the corridor. The open area is delimited by smooth surfaces (walls and glass cabinets) with poor diffraction properties, a situation in which multiple reflections arise frequently. Experimental data have been gathered with a Polaroid sensor placed at 43 known locations, which have been evenly distributed to obtain a good coverage of the environment. At each location, 48 range readings have been obtained by rotating the sensor of 7.5°.

The universal set U is a bitmap of 180×120 square cells of side 0.1 m. Maps are shown as gray-level density plots of U, where white corresponds to $\nu(c) = 0$ and black to $\nu(c) = 1$. A small gray scale is added to each plot.

Figure 4 represents the map produced by the PT approach in 2 min and 48 sec. The uncertainty model (2) has been used, with $R_m = 0.11$ m, $\sigma_a = 2$, $\sigma_\vartheta = 0.08$, $h_1 = 0.055$, $h_2 = 0.078$. The actual profile of the corridor, the entrance, the room and the obstacle are shown in white. In several areas (e.g., $(12, 50)$ and $(95, 95)$) walls are missing and the empty space extends dangerously. The obstacle around $(148, 40)$ gives rise to only a small shadow. Besides, cells located in correspondence of the walls are assigned values of $\nu(c)$ around 0.5. This means that the map building process has been adversely affected by the false reflections, similarly to the observation made for the

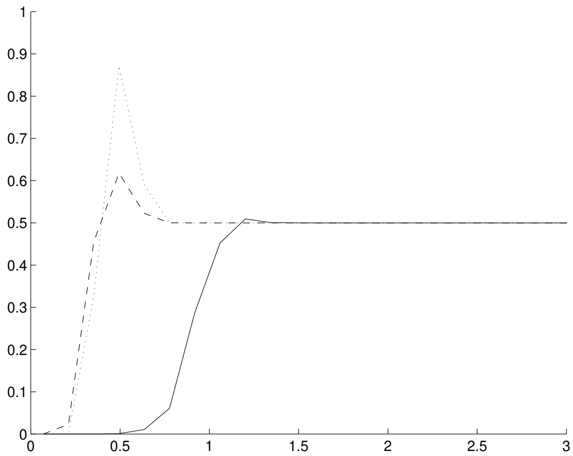

Figure 1: Simulated map obtained with the PT method after the first (dashed), the fourth (dotted) and the fifth (plain) range reading

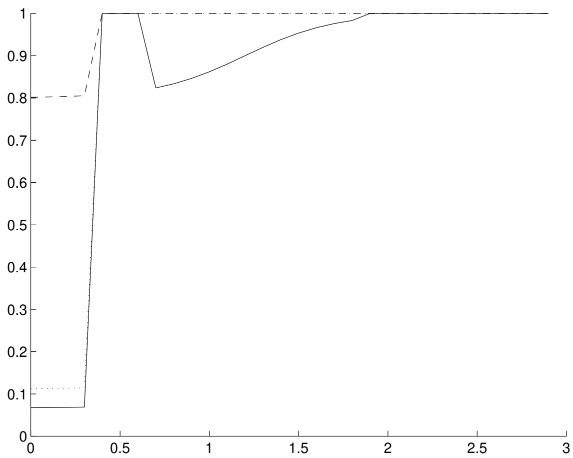

Figure 2: Simulated map obtained with the FL method after the first (dashed), the fourth (dotted) and the fifth (plain) range reading

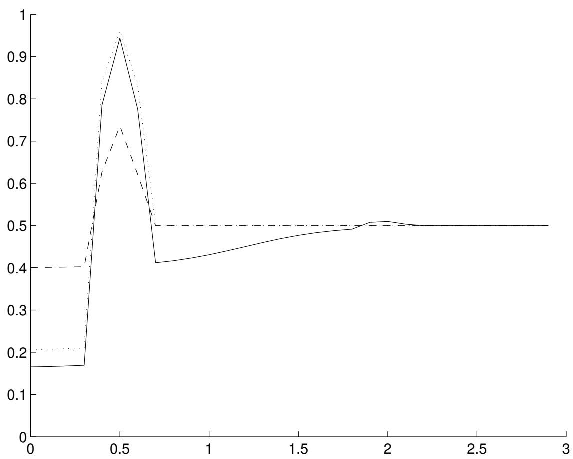

Figure 3: Simulated map obtained with the FM method after the first (dashed), the fourth (dotted) and the fifth (plain) range reading

simulated maps.

The FL method (see Fig. 5) shows the best performance of the three. Here, the uncertainty model was given by the certainty functions (3–5), with $k_e = 0.25$, $k_o = 0.1$, $\Delta r = 0.15$ m, $\rho_v = 1.2$ m. The resulting map is moderately conservative; the corridor appears narrower and the obstacle larger than they are in reality. The room appears rather dim, but the profile of the walls is accurately reconstructed. The small gray areas extending beyond the corridor walls are due to multiple reflections occurring for large angles of incidence. Nevertheless, the algorithm estimated accurately the profile of the walls, by incorporating the range readings obtained for smaller incidence angles. It is worth to remark that FL is the fastest of the three approaches, for it took only 13 sec to compute $\mathcal{N}$.

The map obtained in 31 sec by using the FM algorithm is reported in Fig. 6. Again, the uncertainty model (3–5) was used, but with $k_e = 0.5$, $k_e = 0.05$, $\Delta r = 0.15$ m, $\rho_v = 1$ m. Despite the nice behavior in the simulated map, the experimental results are disappointing. The boundaries are blurred, empty areas extend beyond the walls and the obstacle is just a shadow. In our opinion, however, this result indicates that further analysis is in order.

6 DISCUSSION AND CONCLUSIONS

We have attempted a field comparison of three well known techniques for uncertainty calculus, i.e., probability theory, fuzzy logic and fuzzy measures, by addressing the problem of ultrasonic map building, a relevant task in mobile robotics.

The probabilistic approach, although well established and of great formal elegance, has shown to be very sensitive to outliers and prone to serious errors. This is probably due to the fact that, in order to obtain a computationally feasible algorithm, one is forced to make unrealistic simplifying assumptions. In fact, it has been observed[10] that the zero-order Markov field assumption may induce large errors even in the presence of a slight degree of dependence between the random variables. Indeed, this is the case of map building, since the occupied cells are not evenly distributed, but concentrated in clusters (obstacles). Furthermore, with the maximum entropy initialization the convergence of the Bayesian updating procedure towards an acceptable characterization of the map requires a large number of measures.[17]

A final remark is in order about the choice of the uncertainty model, which was assumed to be Gaussian. This is a reasonable choice in the absence of multiple reflections, but these occur frequently and are difficult to detect. In principle, it should be possible to make the method more robust by using more complicated probability density functions to model the sensor. However, this requires a careful calibration of the model through several preliminary experiments to be performed in the environment.

The best performing method is based on fuzzy logic. The underlying philosophy is completely different; while in the probabilistic approach the sets of empty and occupied cells have sharp boundaries, here the uncertainty is taken into account by modeling these sets as fuzzy. As a consequence, less constraining hypotheses are needed and the designer has more freedom in selecting operators and tools. A possible criticism to this approach is that the membership functions of $\mathcal{E}$ and $\mathcal{O}$ can only increase over time, so that a saturation phenomena may occur on the map. In the presence of dynamic environments, this may be a serious drawback. A solution we are currently exploring is to perform evidence aggregation by using *averaging* operators in place of fuzzy unions.

From a conceptual point of view, the method based on fuzzy measures is probably the most appealing, for it allows to relax the probability axioms while still regarding E and O as crisp sets. However, in our experience, its practical behavior was not as good as expected from the premises.

Since the FM method seems unable to discriminate conflicting information, we intend to take a different viewpoint and regard $m_\emptyset(c)$ as the amount of contradiction that is generated when the various range readings are combined (e.g., in the presence of multiple reflections). This idea[12] leads to a data aggregation procedure that is different from the classical Dempster-Shafer rule, and could prove to be more robust with respect to outliers.

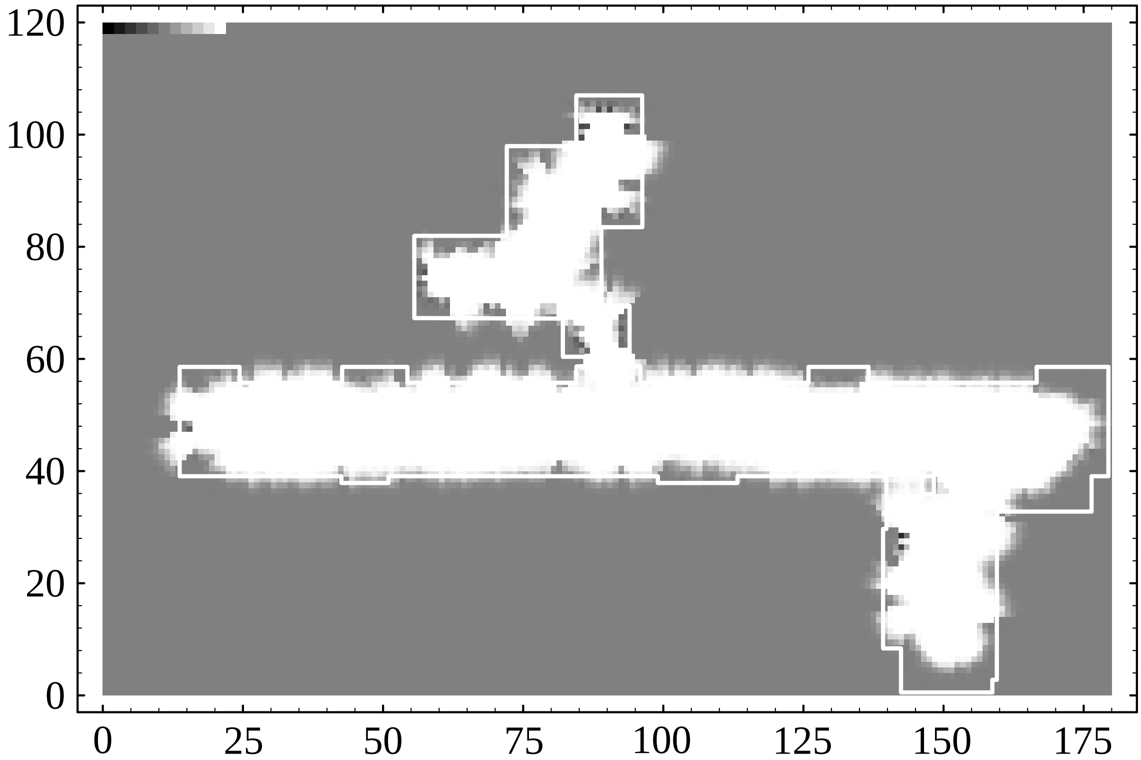

Figure 4: Experimental map obtained with the PT method. The actual profile of the corridor, the entrance, the room and the obstacle are shown in white

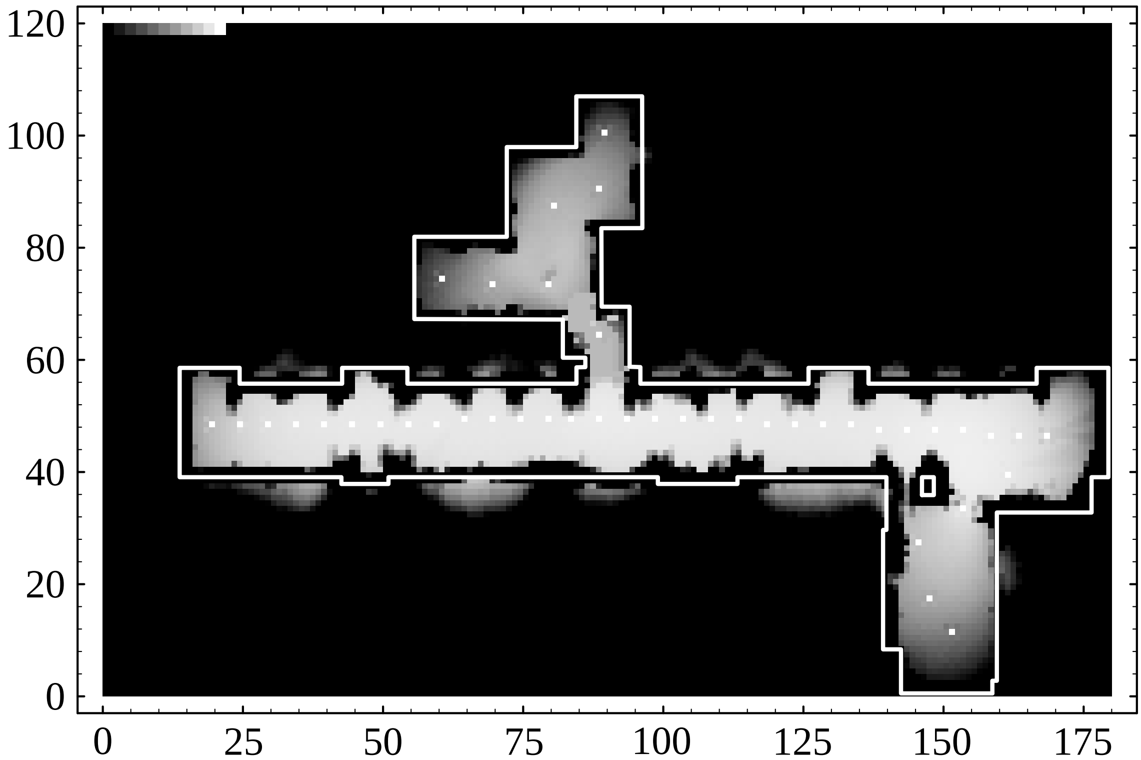

Figure 5: Experimental map obtained with the FL method. White spots indicate the measure points.

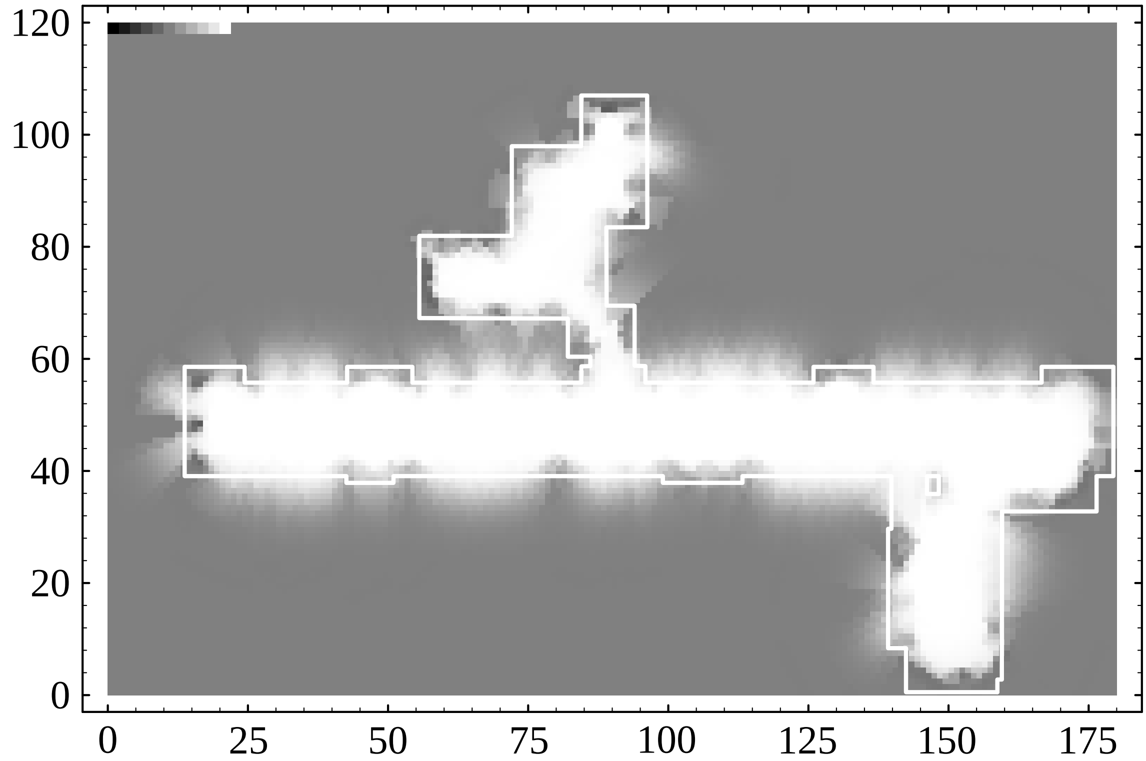

Figure 6: Experimental map obtained with the FM method

ACKNOWLEDGMENTS

This work was partially supported by MURST under 40% funds.

7 REFERENCES

[1] J. J. Leonard and H. F. Durrant-Whyte, *Directed Sonar Sensing for Mobile Robot Navigation*. Kluwer Academic Publishers, 1992.

[2] A. Elfes and H. P. Moravec, "High resolution maps from wide angle sonar," *Proc. 1985 IEEE Int. Conf. on Robotics and Automation*, St. Louis, MO, pp. 116–121, 1985.

[3] A. Elfes, "Occupancy grids: A stochastic spatial representation for active robot perception," in *Autonomous Mobile Robots: Perception, Mapping, and Navigation* (S. S. Iyengar and A. Elfes, eds.), IEEE Computer Society Press, pp. 60–71, 1991.

[4] G. Oriolo, G. Ulivi, and M. Vendittelli, "Motion planning with uncertainty: Navigation on fuzzy maps," *Proc. 4th IFAC Symp. on Robot Control*, Capri, I, pp. 71–78, 1994.

[5] M. Poloni, G. Ulivi, and M. Vendittelli, "Fuzzy logic and autonomous vehicles: Experiments in ultrasonic vision," *Fuzzy Sets and Systems*, no. 69, pp. 15–27, 1995.

[6] G. Oriolo, G. Ulivi, and M. Vendittelli. "On-line map building and navigation for autonomous mobile robots," *Proc. 1995 IEEE Int. Conf. on Robotics and Automation*, Nagoya, J, pp. 2900–2906, 1995.

[7] Klir, G. J., and T. A. Folger, *Fuzzy Sets, Uncertainty and Information*. Prentice-Hall, 1988.

[8] A. P. Tirumalai, B. G. Schunk, and R. C. Jain, "Evidential reasoning for building environment maps," *IEEE Trans. on Systems, Man, and Cybernetics*, vol. 25, no. 1, pp. 10–20, 1995.

[9] J. R. Quinlan, "Consistency and plausible reasoning," *Proc. 8th Int. Joint Conf. on Artificial Intelligence*, Karlsruhe, D, pp. 137–144, 1983.

[10] S. J. Henkind and M. C. Harrison, "An analysis of four uncertainty calculi," *IEEE Trans. on Systems, Man, and Cybernetics*, vol. 18, no. 5, pp. 700–714, 1988.

[11] P. P. Bonissone, "Reasoning, plausible," in *The Encyclopedia of Artificial Intelligence* (S. Shapiro, ed.), 2nd Edition, John Wiley and Sons, pp. 1307–1322, 1991.

[12] D. Dubois, N. P. Wellmann, B. D'Ambrosio, and Ph. Smets, "The nature of unnormalized beliefs encountered in the transferable belief model," *Proc. 8th Conf. on Uncertainty in Artificial Intelligence*, San Matteo, CA, pp. 292–297, 1992.

[13] Polaroid Corporation, *Ultrasonic Ranging System*, 1987.

[14] H. Bandemer and W. Näther, *Fuzzy Data Analysis*. Kluwer Academic Publishers, 1992.

[15] H.-J. Zimmermann, *Fuzzy Set Theory—and Its Applications*. Kluwer Academic Publishers, 1991.

[16] J. Dombi, "A general class of fuzzy operators, the De Morgan class of fuzzy operators and fuzziness measures induced by fuzzy operators," *Fuzzy Sets and Systems*, vol. 8, pp. 149–163, 1982.

[17] S. D. Hill and J. C. Spall, "Sensitivity of a bayesian analysis to the prior distribution," *IEEE Trans. on Systems, Man, and Cybernetics*, vol. 24, no. 2, pp. 216–222, 1994.